IEEE Access
Multidisciplinary | Rapid Review | Open Access Journal

Received February 11, 2022, accepted March 7, 2022, date of publication March 10, 2022, date of current version March 18, 2022.

Digital Object Identifier 10.1109/ACCESS.2022.3158335

Small Signal Stability Analysis and Optimize Control of Large-Scale Wind Power Collection System

LIMEI LI[1], HUI JIANG[2], PEIHONG YANG[2], PENGXIANG FAN[3], PAN QI[2], AND LAN KANG[2]

[1]Hohhot Vocational College, Hohhot 010020, China
[2]School of Information Engineering, Inner Mongolia University of Science and Technology, Baotou 014010, China
[3]Energy Conservation and Environmental Protection Center, Baogang Group, Baotou 014010, China

Corresponding author: Peihong Yang (yph_1025@126.com)

This work was supported in part by the Inner Mongolia Autonomous Region Plan Project of Science and Technology under Grant 2020GG0156 and Grant 2021GG0015, in part by the National Science Foundation of Inner Mongolia Autonomous Region under Grant 2021MS05060, and in part by the Key Laboratory Open Subject of the Ministry of Education under Grant MPSS2021-02.

ABSTRACT The frequency security problem of power system is highlighted as wind power penetration increases yearly, the eigenvalue analysis method based on the deterministic model is difficult to accurately evaluate the small signal stability of power system. The Weibull probability distribution is used to describe the uncertainty of wind speed. In this paper, the shape and scale parameters of the Weibull distribution are calculated by using the maximum likelihood approach and combining with the measured data, and the stability of small signal with large-scale wind power access is analyzed by the probability distribution method. Meanwhile, considering that the lack of inertia of the system caused by high-penetration wind power access can easily lead to the problem of frequency stability, it is proposed to take the maximum damping ratio of regional oscillation mode as optimization objective, virtual inertia and pitch angle control parameters as variables, and frequency stability as constraints, an small signal stability optimization model of wind power access to power system is established according to the proposed probabilistic small signal stability model. The sensitivity algorithm is used to obtain the optimal solution for the virtual inertia and pitch angle control parameters, and the validity of the proposed method and model is verified by two-area four-machine examples. Simulation results show that by optimizing the virtual inertia and pitch angle parameters of wind turbines, the small signal stability of the high-penetration wind power access system can be improved under the condition of ensuring sufficient inertia of the system, which provides a certain theoretical basis for the safe and reliable operation of wind power large-scale cluster access power system.

INDEX TERMS Uncertainty of wind power output, maximum likelihood estimation, small signal stability, virtual inertia, pitch angle control, damping ratio, sensitivity analysis.

I. INTRODUCTION

As a renewable energy source, wind power has attracted much attention from various countries. In recent years, China's wind power industry has developed rapidly and has become one of the major wind power markets in the world. The installed capacity and generation of wind power have risen yearly. By the end of 2020, the cumulative installed capacity of wind power in China has reached 280 million kW. Annual power generation has reached 466.5 billion kW·h [1]. However, the rapid development of large-scale high-penetration wind power has exacerbated the problem of uncertainty in the power system. Meanwhile, as the scale of China's power grid expands and the degree of interconnection deepens, the large-scale clustered grid-connected wind farms have a wider and deeper impact on the stability of the power system. In particular, the small signal stability characteristics of the power system has changed significantly, which will inevitably have an impact on the small signal stability of the system. At present, the small signal instability problems of power system caused by wind power has occurred at home and abroad, which has seriously affected the safe and stable operation of the system [2].

Traditional deterministic analysis methods have been difficult to accurately describe the dynamic behavior of the system after random disturbances when large-scale

The associate editor coordinating the review of this manuscript and approving it for publication was Amjad Ali.

high-penetration wind power is connected to the power system. Therefore, the small signal stability analysis of power system considering the uncertainty of wind power has become a research hotspot of scholars at home and abroad. At present, the small signal stability analysis method of power system considering the uncertainty of wind power mainly includes Monte Carlo method [3], [4], analytic method [5], [6], random response surface method [7]–[9] and point estimation method [10] etc. Among the above methods, Monte Carlo method is the simplest and most accurate, but it is often used to test other algorithms because of its large number of simulations and long time-consuming. Analytic method uses mathematical assumptions and the mathematical derivation is more cumbersome. The random response surface method is used to establish the input and output functions, provided that both their input and output responses are standard normal random variables. While the input of actual wind speed generally does not obey the standard normal distribution. Nataf transformation is usually used to convert the wind speed sequence of non-normal standard distribution into independent standard normal distribution. Point estimation is a probability statistical method based on sample population estimation. The small signal stability analysis of wind power access system has achieved some results. Provides a basis for improving the small signal stability of power system under the wind power access. Reference [11] improved the small signal stability of power system by optimizing the control parameters of rotor side and grid side converter of doubly fed wind turbine, and points out that it is need to dynamically optimize the controller parameters according to wind speed conditions. Reference [12] proposed an optimization algorithm based on teaching and learning to optimize the PI parameters of the wind turbine converter to improve its dynamic performance. Reference [13] proposed to use configured energy storage to improve the stability performance of wind turbines, provide damping for the system under small random disturbances, and enhance the moment inertia of the wind turbines. But configuring energy storage adds cost and control complexity.

However, the traditional generators are constantly replaced by wind turbines, with the increase of wind power penetration yearly, resulting in a continuous reduction in the total inertia of the power system. Therefore, wind power is required to introduce additional control to provide more inertia, so as to improve the frequency stability of the power system. At present, the additional control of wind turbine providing inertia for frequency regulation mainly includes virtual inertia control [14] and pitch angle control [15]. Among them, the wind turbine adopts virtual inertia control when it is under the rated wind speed, which increases the output power response system frequency by releasing rotor kinetic energy. On the other hand, the wind turbine adopts pitch angle control when it is above the rated wind speed, which frequency regulation through the spare output power. The introduction of additional control links can improve the system frequency characteristics, but it will affect the small signal stability of the system [16]–[18]. Reference [19] also pointed out that the introduction of virtual inertia control will deteriorate the small signal stability of the system and reduce the damping ratio in partial oscillation mode. Improper selection of pitch angle control parameters will also affect the small signal stability of the system. By optimizing the PI parameters of pitch angle control link, the damping characteristics of the system can be improved [20], [21].

In fact, under different wind speed conditions, the output characteristics of wind turbines and their effects on small signal stability of power system are also different. Simultaneously, the selection of additional control strategies and parameters are also different. Therefore, the small signal stability mechanism and control strategy of wind power large-scale high-penetration access to the power system are more complex. The existing literature does not consider the optimization of additional control parameters in the full wind speed range to improve the small signal stability of power system. Meanwhile, the frequency stable operation constraint under virtual inertia and pitch angle control are not considered in the optimization modeling and control.

This paper proposes a small signal stability analysis and optimal control strategy of power system in full wind speed range considering large-scale wind power access. Firstly, the parameters of two-parameter Weibull probability distribution model are estimated by maximum likelihood method, and the probability distribution model of wind speed is obtained, based on the measured data of wind speed and wind power of the actual wind farm; Secondly, considering that the lack of inertia of the system caused by high-penetration wind power access can easily lead to the problem of frequency stability, an additional frequency control considering wind power virtual inertia control and pitch angle control in full wind speed range is proposed. A small signal stability optimization model of power system considering system frequency stability constraints is constructed, and the sensitivity algorithm is used to optimize the parameters of virtual inertia control and pitch angle control; Finally, the effects of virtual inertia and pitch angle control parameters on the system damping ratio over the full wind speed range are analyzed through two-area four-machine system as a simulation example. The optimal control parameters of wind turbine are obtained through optimization, and the effectiveness of the proposed method and model is demonstrated.

The remainder of this paper is organized as follows. In Section 2, point estimation is proposed to calculate probabilistic eigenvalues, and describes wind power uncertainty modeling and small signal probabilistic stability analysis. In Section 3, the small signal stability of power system with large-scale high-penetration wind power is studied, including the optimal control of virtual inertia and pitch angle parameters of wind turbine. In Section 4 establish optimization model and algorithm for improving large-scale high-penetration wind power permeability. In section 5, a two-area four-machine system is used as calculation

example to verify the feasibility and effectiveness of the optimal control strategy. Section 6 concludes this paper.

II. WIND POWER UNCERTAINTY MODELING AND SMALL SIGNAL STABILITY ANALYSIS

A. WIND POWER UNCERTAINTY MODELING

This paper proposes to use the two-parameter Weibull distribution to describe the uncertainty characteristics of wind speed considering that the two-parameter Weibull distribution is the most widely used in statistical wind speed distribution, the distribution and probability density functions are as follows:

$$F(v) = 1 - e^{-(\frac{v}{c})^k} \tag{1}$$

$$f(v) = \frac{k}{c}\left(\frac{v}{c}\right)^{k-1} e^{-(\frac{v}{c})^k} \tag{2}$$

where c represents the scale parameter; k represents the shape parameter.

In this paper, the wind speed model for small signal stability analysis is obtained, which based on the historical wind speed observation data of wind farm and used the maximum likelihood method to estimate the two parameters of Weibull distribution model.

In this paper, the histograms of wind speed are obtained by using the wind speed data of a wind farm in Baotou, Inner Mongolia Autonomous Region in 2020. Meanwhile, the wind speed probability density curve of Weibull distribution is obtained by maximum likelihood method. The feasibility of Weibull distribution is verified by comparing the histograms with the probability density curve. Fig. 1 shows the histograms of wind speed measured data and the wind speed probability density fitting curve based on the maximum likelihood method. As can be seen from Fig. 1, the Weibull distribution has higher fitting accuracy and better stability based on the maximum likelihood method, which is also the premise and basis for the formulation of optimal control strategy. It can not only accurately describe the uncertain characteristics of wind speed in wind farms, but also accurately analyze the small signal stability of power systems with large-scale wind power.

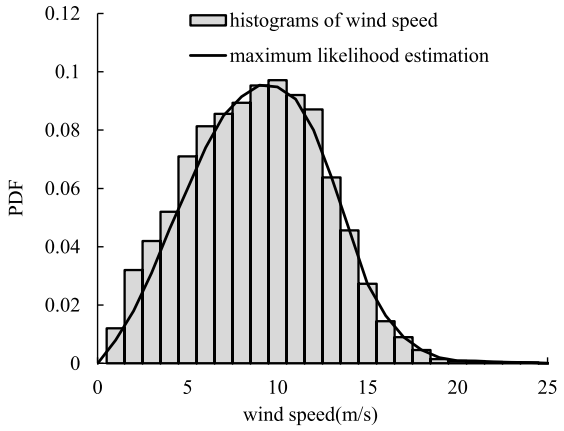

FIGURE 1. Histograms and fitting curves using maximum likelihood estimation of wind speed.

B. STABILITY ANALYSIS OF SMALL SIGNAL PROBABILITY BASED ON POINT ESTIMATION

Point estimation is widely used as a statistical moment method to describe the characteristics of random variables. Compared with the Monte Carlo method, point estimation not only ensures the calculation accuracy, but also has less calculation times. It is an effective method to analyze the uncertainty calculation of wind power. The specific process is as follows:

Assuming that X is a random variable, let $Y = h(X)$ be a nonlinear function with X as the variable. The core idea of the point estimation is to replace $h(X)$ with m probability sets by matching the first few order moments of the function $h(X)$.

The mathematical expectation and the central moment of each order of any point x_i in the sample space $(X_1, X_2, \ldots, X_n)$ are as follows according to the principle of sample approximation.

$$\mu_{ix} = \frac{x_{i1} + x_{i2} + \cdots x_{iN}}{N} \quad i = 1, 2, \cdots, n \tag{3}$$

$$M_{ik} = \frac{(x_{i1} - \mu_{ix})^k + (x_{i2} - \mu_{ix})^k + \cdots (x_{iN} - \mu_{ix})^k}{N} \quad k = 1, 2 \ldots m \tag{4}$$

where m represents the point estimator, generally m takes 2 or 3, that is, 2 point estimation and 3 point estimation.

Expand the Taylor series with $Y = h(X)$ at the mean point μ_i, the formula is as follows:

$$Y = h(\mu_{ix}) + \sum_{i=1}^{n}\sum_{k=1}^{\infty}\frac{1}{k!}\frac{\partial^{(k)}}{\partial x}h(\mu_{ix})(x_i - \mu_i)^k \tag{5}$$

The mathematical expectation of Y can be expressed as:

$$E(Y) = h(\mu_{ix}) + \sum_{k=1}^{\infty}\frac{1}{k!}[\frac{\partial^k h(\mu_{ix})}{\partial x}]M_{ik}(x) \quad (i = 1, 2, \cdots n, \quad k = 1, 2, \cdots 2m-1) \tag{6}$$

Let m estimated points $x_{ij}(i = 1, 2, \ldots, n, j = 1, 2, \ldots, m)$ are extracted from the n-dimensional random variable $X = \{X_1, X_2, \ldots, X_n\}$, and together with the mean values of other variables, a point estimation group $(\mu_{1x}, \mu_{2x}, \cdots x_{ij}, \cdots \mu_{(n-1)x}, \mu_{nx})$ is formed. The weight of each group estimation points is P_{ij}, and the weight of each random variable is equal, that is:

$$\begin{cases} \sum_{j=1}^{m} P_{ij} = \frac{1}{n} \\ \sum_{i=1}^{n}\sum_{j=1}^{m} P_{ij} = 1 \end{cases} \tag{7}$$

If x_{ij} satisfies

$$\sum_{i=1}^{n}\sum_{j=1}^{m}(x_{ij} - \mu_{ix})^k = \mathrm{M}_{ik} \tag{8}$$

Then x_{ij} and p_{ij} can completely match the mathematical expectation of outputting random variables,

$$E(y) = \sum_{i=1}^{n}\sum_{j=1}^{m} P_{ij}h(\mu_{1x}, \cdots x_{ij}, \cdots, \mu_{(n-1)x}, \mu_{nx}) + h^k(.) \tag{9}$$

where $h^k(.)$ $(k = 2\mathrm{m}, 2\mathrm{m}+1, \cdots, \infty)$ represents the higher-order Taylor series expansion term. If the higher-order term is omitted, the following formula can be obtained

$$E(y) = \sum_{i=1}^{n}\sum_{j=1}^{m} p_{ij}h(\mu_{1x}, \cdots x_{ij}, \cdots, \mu_{(n-1)x}, \mu_{nx}) \tag{10}$$

By the same token, the m-order moment of y can be obtained, the formula is as follows:

$$E(y^m) = \sum_{i=1}^{n}\sum_{j=1}^{m} p_{ij}h(\mu_{1x}, \cdots x_{ij}, \cdots, \mu_{(n-1)x}, \mu_{nx})^m \tag{11}$$

The probability distribution is obtained by series expansion method after obtaining the moments of random variable X. Take the probability distribution function of the output random variable x_j as $F_j(x_j)$, the expectation and variance are μ_{xj} and σ_{xj} respectively, the standardized form of the random variable is:

$$x_j^* = \frac{x_j - \mu_{xj}}{\sigma_{xj}} \tag{12}$$

Let the quantile of x^* is a, then the third order standardized semi-invariants of $x_j^*(a)$ can be approximately expressed as:

$$\begin{aligned} x_j^*(a) = {} & \Phi^{-1}(a) + \frac{1}{6}(\Phi^{-1}(a)^2 - 1)K_3 \\ & + \frac{1}{24}(\Phi^{-1}(a)^3 - 3\Phi^{-1}(a))K_4 \\ & + \frac{1}{120}(\Phi^{-1}(a)^4 - 6\Phi^{-1}(a)^2 + 3)K_5 \end{aligned} \tag{13}$$

where $\Phi^{-1}(a) = \int_{-\infty}^{a}\Phi(x)\mathrm{d}x$, $\Phi(x)$ represents the probability density function of the standard normal distribution; K_i represents the j-th order semi-invariant, which can be obtained by the semi-invariant and the origin moment:

$$\begin{cases} K_1 = m_1 \\ K_i = m_i - \sum_{k=1}^{m}\binom{i-1}{k} m_k K_{i-k} (i \geq 2) \end{cases} \tag{14}$$

Finally, the probability distribution of the random variable x_j can be obtained by formula (15).

$$x_j(a) = x_j^*(a)\sigma_{xj} + \mu_{xj} \tag{15}$$

III. VIRTUAL INERTIA AND PITCH ANGLE CONTROL PARAMETERS OPTIMIZATION

As the operating condition of wind turbine is closely related to the wind speed of wind farm, virtual inertia and pitch angle control are used to response system frequency. Generally, the virtual inertia control is used when the wind turbine is operating below the rated wind speed; The pitch angle control is used when the wind turbine is operating at the rated wind speed and above, which can realize the frequency response control in the full wind speed range. Therefore, this paper optimizes the parameters of the virtual inertia and pitch angle control link respectively to improve the small signal stability of the power system according to the operating conditions of wind turbines. The structural block diagram of virtual inertia and pitch angle control of frequency response is shown in Fig. 2.

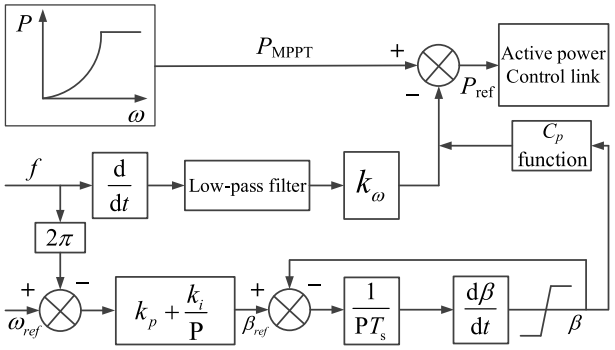

FIGURE 2. Structure diagram of virtual inertia and pitch angle control.

A. VIRTUAL INERTIA CONTROL PARAMETER OPTIMIZATION

On the premise of meeting the system frequency stability, the virtual inertia control parameters are optimized to enhance the small signal stability of the power system. Taking the maximum damping ratio of the power system oscillation mode as the objective, the virtual inertia control parameters as the optimization variables, the frequency stability as the constraint condition, to establish the optimization model. The optimization results can ensure not only the system frequency stability, but also the small signal stability in the operation of the wind turbine. The dynamic equation of the wind turbine is as follows [19]:

$$2H_\omega\dot{\omega} = P_{\mathrm{MPPT}} - P_s \tag{16}$$

where H_ω represents the equivalent inertia of virtual inertia control; P_{MPPT} represents the maximum power tracking output of wind turbine; P_{s} represents the stator output power of wind turbine.

The equivalent inertia H_ω can be expressed as:

$$H_\omega = \frac{k_\omega}{4\pi} \tag{17}$$

where k_ω represents the virtual inertia control parameter, which is one of the parameters optimized in this paper.

Under the virtual inertia control, the frequency stability of the system is related to the total inertia provided by the wind farm. The total inertia of the wind farm can be calculated

by equation (18):

$$H_{WF} = \frac{\sum_{n=1}^{N} H_{\omega,n} S_{DFIG,n}}{\sum_{n=1}^{N} S_{DFIG,n}} \tag{18}$$

In order to ensure the stability of system frequency during parameter optimization.

$$H_{WF} \geq H_{\min} \tag{19}$$

where $H_{\min}$ represents the minimum value of the total inertia of the wind farm required by the system.

Further we can obtain

$$\sum_{n=1}^{N} k_{\omega,n} S_{DFIG,n} \geq 4\pi H_{\min} \sum_{n=1}^{N} S_{DFIG,n} \tag{20}$$

Meanwhile, the constraints for small signal stability should be considered to obtain all eigenvalues with positive damping, that is, during the optimization of parameters, it is necessary to ensure that the damping ratio is greater than 0 for all oscillation modes.

$$\zeta_j > 0 \quad (j = 1, 2, \cdots m) \tag{21}$$

where m represents the number of system damping ratios.

In summary, the optimized model of the virtual inertia control parameters can be obtained as follows:

$$\begin{cases} \max & \zeta \\ \text{s.t.} & \zeta_j > 0 \\ & \sum_{n=1}^{N} k_{\omega} S_{DFIG,n} \geq 4\pi H_{\min} \quad \sum_{n=1}^{N} S_{DFIG,n} \\ & k_{\omega,n}^{\min} \leq k_{\omega,n} \leq k_{\omega,n}^{\max} \end{cases} \tag{22}$$

B. PITCH ANGLE CONTROL PARAMETERS OPTIMIZATION

Pitch angle control can not only effectively adjust the output power of wind turbine, but also benefit the frequency response of wind turbine. Under the premise of frequency stability, the small signal stability of the system can be improved by optimizing the PI parameters (k_p and k_I) of the pitch angle control link. This paper mainly analyzes the influence of wind turbine on small signal stability. In the analysis process, it is considered that the output power of synchronous unit remains unchanged. Meanwhile, in order to ensure the small signal stability in the PI parameter optimization process, two indicators of the eigenvalue real part δ and the damping ratio ζ are proposed as the constraints of the optimization model, as shown in equation (23):

$$\begin{cases} \zeta \geq \zeta_{\min} \\ \delta \leq \delta_{\max} \end{cases} \tag{23}$$

where ζ_{min} and δ_{max} represent the minimum limit of the damping ratio and the maximum limit of the real part of the eigenvalue set in the optimization process.

The constraint equation of the real part of the eigenvalue δ established in the formula (23) is to prevent the instability of the system from being induced by the small value of δ [22].

The unequal constraint of the equation (23) can be obtained by first-order sensitivity linearization:

$$\begin{cases} \zeta(\gamma_0) + \sum \frac{\partial \zeta(\gamma_0)}{\partial \gamma} \Delta\gamma \geq \zeta_{\min} \\ \delta(\gamma_0) + \sum \frac{\partial \delta(\gamma_0)}{\partial \gamma} \Delta\delta \leq \delta_{\max} \end{cases} \tag{24}$$

where γ represents the controllable parameter; $\zeta(\gamma_0)$ and $\delta(\gamma_0)$ represent initial values; $\partial\zeta/\partial\gamma$ and $\partial\delta/\partial\gamma$ represent the sensitivity of ζ and δ to γ, respectively; $\Delta\zeta$ and $\Delta\delta$ represent the variations of ζ and δ.

In order to reduce the influence on stability during the optimization of PI parameters, the objective function of equation (25) is established.

$$\min F = w_p \sum_{n=1}^{N} \left|\Delta k_{pn}\right| + w_I \sum_{n=1}^{N} \left|\Delta k_{In}\right| \tag{25}$$

where Δ represents the variation; k_{pn} and k_{In} represent the n-th wind turbine PI controller parameters; N represents the number of generators; w_p and w_I represent the weight of the corresponding parameters, respectively.

According to equations (24)-(25), the sensitivity of eigenvalues dominated by PI parameters to control parameters is formed into a new constraint equation, and the optimization model of pitch angle control parameters is established as follows:

$$\begin{cases} \max & F \\ \text{s.t.} & \zeta_0 + \sum_{n=1}^{N} \left(\frac{\partial \zeta(\zeta_0)}{\partial k_{pn}} \Delta k_{pn} + \sum_{n=1}^{N} \left(\frac{\partial \zeta(\zeta_0)}{\partial k_{In}} \Delta k_{In}\right) \geq \zeta_{\min}\right. \\ & \delta_0 + \sum_{n=1}^{N} \left(\frac{\partial \delta(\delta_0)}{\partial k_{pn}} \Delta k_{pn} + \sum_{n=1}^{N} \left(\frac{\partial \delta(\delta_0)}{\partial k_{In}} \Delta k_{In}\right) \leq \delta_{\max}\right. \\ & k_{p,n}^{\min} \leq k_{p,n} \leq k_{p,n}^{\max} \\ & k_{I,n}^{\min} \leq k_{I,n} \leq k_{I,n}^{\max} \end{cases} \tag{26}$$

Meanwhile, in the control parameter optimization model, the constraints should also include the power balance of the system and unequal constraint equations for the output limits of each device.

IV. OPTIMIZATION ALGORITHMS

In this paper, the small signal stability constrained optimal power flow (SC-OPF) [23] based on eigenvalue sensitivity is used to optimize the virtual inertia and pitch angle control parameters. Point estimation is used to analyze the small signal stability probability, and compared with the non-optimized parameters to verify the effectiveness and feasibility of the method proposed in this paper. The algorithm flowchart is shown in Fig. 3.

As shown in Fig. 3, the whole calculation process is divided into four steps, namely initial value calculation, parameter

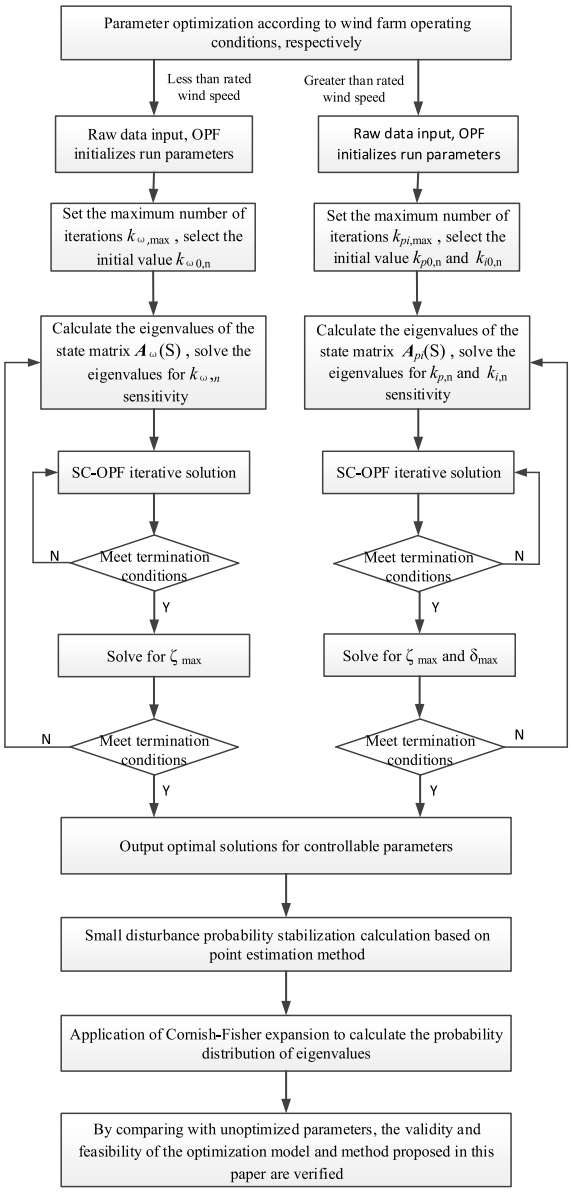

FIGURE 3. Flowchart of optimization algorithm.

optimization, termination judgment, and probability analysis. The initial value calculation includes operation initial value and given data of the OPF, where the initial value of the OPF is selected from the power flow calculation results, and the given data includes the number of iterations, optimization parameters initial value, and termination conditions.

The sensitivity of the oscillation mode damping ratio to the virtual inertia parameters is used in the virtual inertia parameter optimization process. The specific calculation formulas are shown in equations (27)-(28).

$$\frac{\partial \zeta}{\partial k_\omega} = \frac{-\omega^2 \mathrm{Re}(\frac{\partial \lambda}{\partial k_\omega}) + \delta\omega \mathrm{Im}(\frac{\partial \lambda}{\partial k_\omega})}{|\lambda^3|} \tag{27}$$

$$\frac{\partial \lambda}{\partial k_\omega} = \frac{\boldsymbol{v}^{\mathrm{T}} \frac{\partial \boldsymbol{A}}{\partial k_\omega} \boldsymbol{u}}{\boldsymbol{v}^{\mathrm{T}} \boldsymbol{u}} \tag{28}$$

where $\boldsymbol{A}$ represents the state matrix; $\boldsymbol{v}$ represents the left eigenvector of the oscillation mode; $\boldsymbol{u}$ represents the right eigenvector of the oscillation mode.

For the termination condition, the virtual inertia control takes the maximum the damping ratio ζ as the objective. By setting the number of iterations, the damping ratio obtained at the l-th time is $\zeta_{\max}^{l}$ and the $l+1$-th time is $\zeta_{\max}^{l+1}$. By comparing as the termination criterion, that is $\left|\zeta_{\max}^{l+1} - \zeta_{\max}^{l}\right| \leq \varepsilon_\omega$, where ε_ω is an arbitrary constant set according to the need of optimization calculation. The pitch angle control takes the minimum fluctuation of the optimized parameters as the objective, with the minimum value of the damping ratio ζ and the maximum value of the real part of the modal eigenvalue δ as constraints, the termination conditions are $\left|k_p^{l+1} - k_p^{l}\right| \leq \varepsilon_p$ and $\left|k_I^{l+1} - k_I^{l}\right| \leq \varepsilon_I$, where ε_p and ε_I are arbitrary constants set according to the needs of the optimization calculation.

After obtaining the optimization parameters for virtual inertia and pitch angle control, the probabilistic small signal stability calculation of the power system containing wind power is calculated and still analyzed for two operating conditions, that is, operation under rated wind speed and rated wind speed and above. The probability distribution characteristics of the eigenvalues are analyzed under two operating conditions and compared with the non-optimized parameters (initial values of parameters) to verify the effectiveness of the model and method proposed in this paper.

V. EXAMPLE ANALYSIS

In this paper, a typical IEEE two-area four-machine system is used as calculation example for simulation calculations. The original system structure is modified considering the access of large-scale wind turbines. The wiring schematic is shown in Fig. 4, and the with specific parameters are in [24].

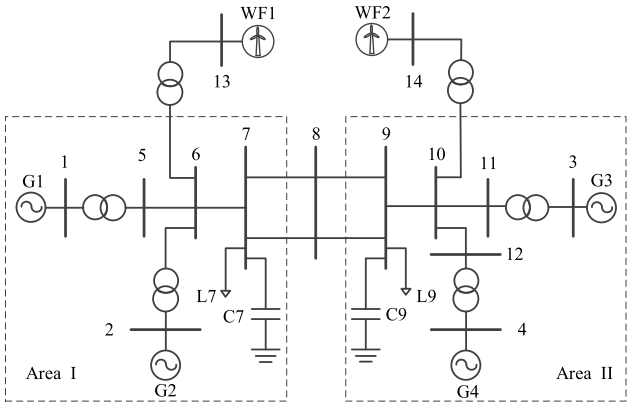

FIGURE 4. Small signal stability test system with DFIG.

As can be seen from Fig.4, the two wind farms are connected to the bus 6 and the bus 10 respectively. In this paper, the parameters of wind farm are optimized under the two operating conditions of virtual inertia control and pitch angle control, due to the different participation in system

frequency regulation. Therefore, an equivalent fan which from the wind farm is involved in the calculation. The small signal stability of wind farm access is optimized which can be divided into four scenarios according to the wind speed of the wind farm, because the two wind farms are connected to area I and area II respectively. Since the rated wind speed of wind turbine is 12.5m/s, two typical wind speeds are selected for calculation, as shown in Table 1.

TABLE 1. Simulation calculation scenarios.

Scenarios	P_{WF1}(MW)	P_{WF2}(MW)	v_{WF1}(m/s)	v_{WF2}(m/s)
I	300	300	9	9
II	300	300	15	15
III	300	300	9	15
IV	300	300	15	9

Before calculation, parameters initialization is required where the virtual inertia control link $k_{\omega,1}^{\min} = k_{\omega,2}^{\min} = 0$, $k_{\omega,1}^{\max} = k_{\omega,2}^{\max} = 2.5$, $H_{\min} = 2.84$, $k_{\omega 0,1} = k_{\omega 0,2} = 1$; Number of iterations $l_{\omega,\max} = 20$; Pitch angle control link $k_{p,1}^{\min} = k_{p,2}^{\min} = 0, k_{I,1}^{\min} = k_{I,2}^{\min} = 0$, $k_{p,1}^{\max} = k_{p,2}^{\max} = 4$, $k_{I,1}^{\max} = k_{I,2}^{\max} = 0.5$, Number of iterations $l_{pI,\max} = 20$, $k_{p0,1} = k_{p0,2} = 1$, $k_{I0,1} = k_{I0,2} = 0.1$, $w_p = 1/k_{p,0}$, $w_I = 1/k_{I,0}$, $\varepsilon_\omega = 10^{-6}$, $\varepsilon_p = \varepsilon_I = 10^{-3}$.

Among them, the initial values of the optimization parameters are derived from [15]. Meanwhile, G1 is taken as the slack bus, G2, G3, and G4 are PQ nodes in the calculation, and the load remains unchanged.

A. PARAMETER OPTIMIZATION

1) SCENARIO I

In scenario I, the wind farms in region I and region II operate below the rated wind speed, so only the parameters of the virtual inertia link need to be optimized. Table 2 gives the oscillation modes before parameter optimization.

TABLE 2. Calculated results of oscillatory modes before.

Oscillation mode	Eigenvalue	Damping ratio (%)
Local oscillation	-0.1632±j4.4383	3.6746
	-0.1541±j3.5841	4.2956
Regional oscillation	-0.0591±j3.7216	1.5878

As can be seen from Table 2 that the damping in the regional oscillation mode is relatively small, which is an optimization objective. While preventing the optimization of the regional damping ratio, reduce the damping ratio of the local oscillation model, and set all the damping in the system to be greater than 3.

Fig. 5 shows the variation of the control parameters $k_{\omega 1}$ and $k_{\omega 2}$ with the interval damping ratio. As can be seen

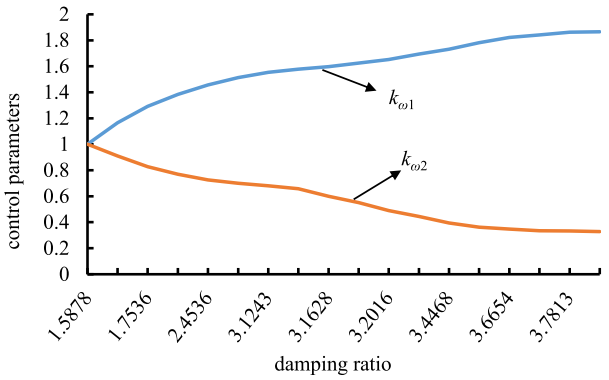

FIGURE 5. Virtual inertia control parameter optimization process.

from Fig. 5, $k_{\omega 1}$ increases continuously and finally tends to be stable when the value increases to about 1.8, while $k_{\omega 2}$ decreases continuously until it tends to be stable. At this time, the optimal solution of damping ratio $\varepsilon_\omega = 8 \times 10^{-7}$, optimum solution $k_{\omega 1} = 1.865$, $k_{\omega 2} = 0.328$. Table 3 gives the damping ratio changes before and after optimization and the analysis results.

TABLE 3. Comparison of calculation results before and after parameter optimization.

	Damping ratio ζ(%)	$\partial\zeta/\partial k_{\omega 1}$	$\partial\zeta/\partial k_{\omega 2}$
Before optimization	1.5878	1.26×10^{-2}	3.24×10^{-3}
After optimization	3.7854	-5.68×10^{-3}	-9.53×10^{-2}

2) SCENARIO II

In scenario II, the wind farms in region I and region II operate above the rated wind speed, so only the parameters of the pitch angle link need to be optimized. Table 4 shows the oscillation mode before the parameter optimization.

TABLE 4. Oscillation mode calculation results before scenario II parameter optimization.

Oscillation mode	Eigenvalue	Damping ratio (%)
Local oscillation	-0.1582±j4.4218	3.5754
	-0.1497±j3.5643	4.1963
Regional oscillation	-0.0532±j3.7683	1.4116

As can be seen from Table 4, compared with the calculation results in Table 2, the damping ratios of the three oscillation modes are not significantly different and slightly decrease. When the pitch angle control parameters are optimized, set the minimum threshold of the damping ratio $\zeta_{\min} = 0.03$, eigenvalue real part maximum $\delta_{\max} = -0.01$. The optimal values of k_{p1}, k_{p2}, k_{i1}, and k_{i2} are calculated

and optimized according to the maximum number of iterations according to the given initial value of PI parameters and equation (26). Among them, the convergence criterion is calculated when the calculation results of Δk_p and Δk_I are both less than 10^{-3}, and the optimal value is output. Fig. 6 shows the variation of pitch angle control parameters and interval damping ratio, where the damping ratio reaches 3.8521.

Fig. 6 shows the optimal solution of the iterative process of control parameters.

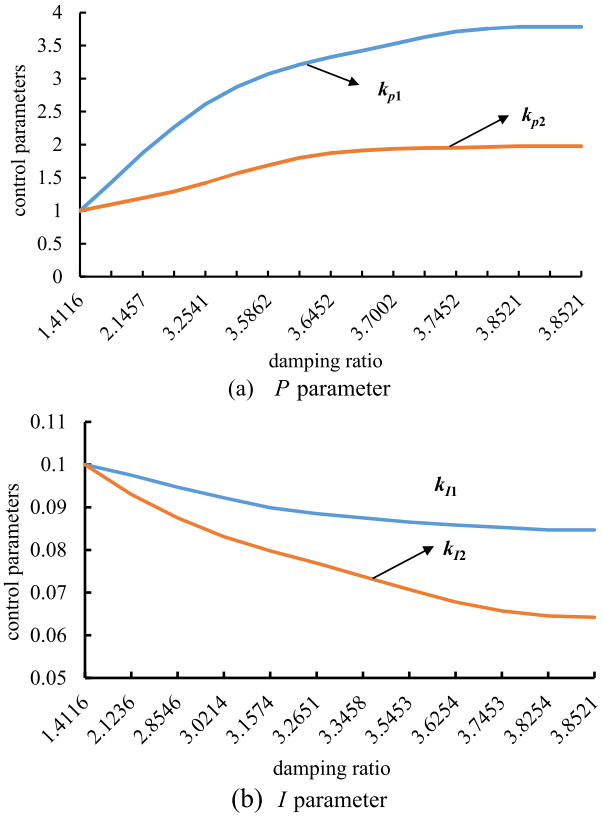

FIGURE 6. Pitch angle control parameter optimization process.

In Fig. 6 the calculation process is as follows:

$$\begin{cases} k_{p1}^{l+1} = k_{p1}^{l} + \Delta k_{p1}^{l} \\ k_{p2}^{l+1} = k_{p2}^{l} + \Delta k_{p2}^{l} \\ k_{I1}^{l+1} = k_{I1}^{l} + \Delta k_{I1}^{l} \\ k_{I2}^{l+1} = k_{I2}^{l} + \Delta k_{I2}^{l} \end{cases} \tag{29}$$

In Equation (29), after the first iteration of calculation and the initial value is added to form the new calculated value, and determine whether the convergence criterion is satisfied, if not, continue to iterate until the convergence condition is satisfied, i.e., the calculated parameter variation is less than 10^{-3}. If the maximum number of iterations still does not meet the convergence conditions, the eigenvalue matrix and sensitivity are recalculated again until the condition is met, and the final optimal value is output.

Table 5 gives the variation of damping ratio before and after optimization and the analysis results.

TABLE 5. Comparison of calculation results before and after parameter optimization.

α	$\partial\zeta/\partial\alpha$	$\partial\delta/\partial\alpha$	Optimum value
$k_{p,1}$	-7.121×10^{-3}	0.03217	3.7831
$k_{p,2}$	-4.853×10^{-3}	0.05421	1.9758
$k_{I,1}$	3.217×10^{-4}	-8.7541	0.0847
$k_{I,2}$	2.351×10^{-4}	-12.5422	0.0642

As can be seen from Table 5, the sensitivity of the damping ratio ζ to the parameter k_p is greater than k_I, and k_p parameter plays a major role in the regulation process consistent with the results shown in Fig. 6, which means the optimization process is correct and reasonable. The sensitivity of the real part of the eigenvalue δ to the parameter k_I is greater than k_p, indicating that the parameter k_I has a greater effect on adjusting δ.

3) SCENARIOS III AND IV

The different wind speeds of the two wind farms are analyzed in scenarios III and IV. One of the wind farms is operating above the rated wind speed, and the other is operating below the rated wind speed. During parameter optimization, the virtual inertia and pitch angle control parameters need to be optimized simultaneously. Considering that the virtual inertia control and pitch angle control parameters have been optimized for Scenarios I and II, therefore, the optimal values of Scenarios I and II are taken as the initial values for Scenarios III and IV parameter optimization. This chapter only gives the calculation results of the oscillation mode before the parameter optimization under Scenario III, and the calculation results of the oscillation mode in Scenario IV are not listed. The calculation results of scenario III are shown in Table 6.

As can be seen from Table 6, the damping under Scenario III is also the smallest under the regional oscillation mode, and in a weakly damped state, which is unfavorable to the safe and stable operation of the system. The damping ratio of the system is improved by optimizing the parameters, and the optimization results are shown in Table 7.

The optimization results for Scenario IV are obtained in the same way, as shown in Table 8.

B. SMALL SIGNAL PROBABILITY STABILITY ANALYSIS

During the small signal probabilistic stability analysis and calculation, the cumulative distribution of wind speed shown in Fig. 2 is used as input for wind farms I and II, and the small signal probabilistic stability results are analyzed using point estimation. When the parameters are non-optimized, the parameters of the virtual inertia control link and the pitch angle control link take the initial values. After the parameters are optimized, the parameters take the average of the

TABLE 6. Scenario III oscillation mode calculation results before parameter optimization.

Oscillation mode	Eigenvalue	Damping ratio (%)
Local oscillation	-0.1621±j4.4264	3.6597
	-0.1502±j3.5894	4.1809
Regional oscillation	-0.0563±j3.7892	1.4856

TABLE 7. Scenario III parameter optimization results.

$k_{\omega 1}$	$k_{p,2}$	$k_{I,2}$	ζ
1.623	2.123	0.0697	3.8546

TABLE 8. Scenario IV parameter optimization results.

$k_{p,1}$	$k_{I,1}$	$k_{\omega 2}$	ζ
3.964	0.0852	0.295	3.7621

optimized calculation results of the four scenarios, as shown in Table 9.

TABLE 9. Optimization parameters for stable calculations with small signal probability.

$k_{\omega 1}$	$k_{\omega 2}$	$k_{p,1}$	$k_{I,1}$	$k_{p,2}$	$k_{I,2}$
1.744	0.312	3.874	0.849	2.049	0.067

The comparison results of the expected values and standard deviations of the real and imaginary parts of the eigenvalues of the three oscillation modes before and after the parameter optimization are obtained by calculation, as shown in Table 10.

TABLE 10. Expected value and standard deviation of eigenvalues.

(A). EXPECTED VALUE AND STANDARD DEVIATION OF EIGENVALUES BEFORE PARAMETER OPTIMIZATION

Oscillation mode	Real part		Imaginary part	
	Expected value	Standard deviation	Expected Value	Standard deviation
Local	-0.1532	0.0024	4.3271	0.0037
Local	-0.1476	0.0082	3.6013	0.1021
Regional	-0.0573	0.0141	3.8435	0.0194

(B). EXPECTED VALUE AND STANDARD DEVIATION OF EIGENVALUES AFTER PARAMETER OPTIMIZATION

Oscillation mode	Real part		Imaginary part	
	Expected value	Standard deviation	Expected value	Standard deviation
Local	-0.1578	0.0028	4.2833	0.0042
Local	-0.1493	0.0103	3.6452	0.094
Regional	-0.1423	0.0203	3.5982	0.0173

As can be seen from Table 10 that through parameter optimization, the expected value and standard deviation of the local eigenvalues have not changed much, while the expected value and standard deviation of the real part of the regional eigenvalues have changed greatly. The expected value of the real part has been significantly improved, while the expected value of the imaginary part of eigenvalues has not changed much, and slightly decreased. By comparing the expected values and standard deviations of the real and imaginary parts of the eigenvalues, the small signal stability of the system has been improved to some extent after optimization, which is conducive to the stable operation of the system.

Through the above analysis, the regional damping ratio in this calculation example is relatively small and weak, which is not conducive to the stable operation of the system. After parameter optimization, the damping ratio is effectively improved. Fig. 7 shows the comparison of the cumulative distribution of the regional damping ratio before and after parameter optimization.

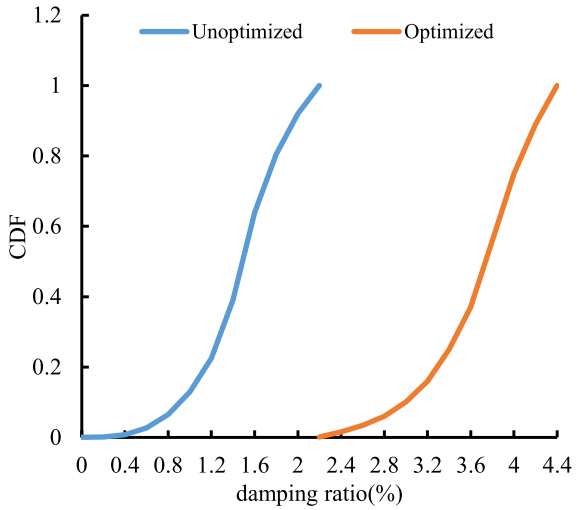

FIGURE 7. Comparison of cumulative distribution results of damping ratio.

As can be seen from Fig. 7 that after parameter optimization, the cumulative distribution curve of system damping ratio has changed greatly, and the damping ratio has increased significantly. It also further shows that after virtual inertia and pitch angle control, the small signal stability of power system with wind farm has been significantly improved. The obtained results are more scientific and reasonable considering the small signal probabilistic stability analysis of the wind farm operation uncertainty, which can verify and illustrate the correctness of the proposed method and model in this paper.

VI. CONCLUSION

This paper proposes a small signal probabilistic stability analysis method based on measured data, which can scientifically characterize the small signal stability of power systems with large-scale wind power access. Taking into account the annual increase in wind power penetration, the idea of combination control of virtual inertia and pitch angle is proposed, and the frequency stability of the system and turbine operation stability are fully considered in the control process.

The parameter optimization model is established, an optimization algorithm based on sensitivity analysis is proposed, and the two-area four-machine system is used as calculation example to analyze the optimization process of virtual inertia control and pitch angle control parameters through four scenarios. Last, the probabilistic small signal stability analysis method is used to verify the effectiveness and accuracy of proposed optimization model and algorithm.

In this paper, only two given wind speeds are optimized, and the capacity of the wind farm is 300 MW. The effect of wind speed and wind farm capacity variation on parameter optimization and damping ratio will be investigated further.

REFERENCES

[1] China Electricity Council. *2021 China's Electricity Industry Annual Report 2021*. Accessed: Jul. 8, 2021. [Online]. Available: https://cec.org.cn/detail/index.html?3-298413

[2] W. Wang, C. Zhang, G. He, G. Li, J. Zhang, and H. Wang, "Overview of research on subsynchronous oscillations in large-scale wind farm integrated system," *Power Syst. Technol.*, vol. 41, no. 4, pp. 1050–1060, 2017.

[3] J. L. Rueda, D. G. Colome, and I. Erlich, "Assessment and enhancement of small signal stability considering uncertainties," *IEEE Trans. Power Syst.*, vol. 24, no. 1, pp. 198–207, Feb. 2009.

[4] T. R. Ayodele, "Analysis of Monte Carlo simulation sampling techniques on small signal stability of wind generator-connected power system," *J. Eng. Sci. Technol.*, vol. 11, no. 4, pp. 563–583, Apr. 2016.

[5] J. Luo, L. Shi, and Y. Ni, "A solution of optimal power flow incorporating wind generation and power grid uncertainties," *IEEE Access*, vol. 6, pp. 19681–19690, 2018.

[6] J. R. Hockenberry and B. C. Lesieutre, "Evaluation of uncertainty in dynamic simulations of power system models: The probabilistic collocation method," *IEEE Trans. Power Syst.*, vol. 19, no. 3, pp. 1483–1491, Aug. 2004.

[7] Y. Zhou, Y. Li, W. Liu, D. Yu, Z. Li, and J. Liu, "The stochastic response surface method for small-signal stability study of power system with probabilistic uncertainties in correlated photovoltaic and load," *IEEE Trans. Power Syst.*, vol. 32, no. 3, pp. 4551–4559, Feb. 2004.

[8] W. Du, H. Wang, and S. Bu, "Probabilistic analysis of small-signal stability of a power system affected by grid-connected wind power generation," Tech. Rep., 2018.

[9] Z. Ren, W. Li, R. Billinton, and W. Yan, "Probabilistic power flow analysis based on the stochastic response surface method," *IEEE Trans. Power Syst.*, vol. 31, no. 3, pp. 2307–2315, May 2016.

[10] P. Kanyingi, K. Wang, G. Li, and W. Wu, "A robust pair copula-point estimation method for probabilistic small signal stability analysis with large scale integration of wind power," *J. Clean Energy Technol.*, vol. 5, no. 2, pp. 85–94, 2017.

[11] Y. Jia, T. Huang, Y. Li, and R. Ma, "Parameter setting strategy for the controller of the DFIG wind turbine considering the small-signal stability of power grids," *IEEE Access*, vol. 8, pp. 31287–31294, 2020.

[12] S. Chatterjee, A. Naithani, and V. Mukherjee, "Small-signal stability analysis of DFIG based wind power system using teaching learning based optimization," *Electr. Power Energy Syst.*, vol. 78, pp. 672–689, Jun. 2016.

[13] O. Cornea, D. Hulea, N. Muntean, and G.-D. Andreescu, "Step-down switched-inductor hybrid DC-DC converter for small power wind energy conversion systems with hybrid storage," *IEEE Access*, vol. 8, pp. 136092–136107, 2020.

[14] P. H. Yang, B. He, B. Wang, and X. L. Dong, "Coordinated control of rotor kinetic energy and pitch angle for large-scale doubly fed induction generators participating in system primary frequency regulation," *IET Renew. Power Gener.*, vol. 15, no. 8, pp. 1836–1847, 2021.

[15] P. Yang, X. Dong, Y. Li, L. Kuang, J. Zhang, B. He, and Y. Wang, "Research on primary frequency regulation control strategy of wind-thermal power coordination," *IEEE Access*, vol. 7, pp. 144766–144776, 2019.

[16] J. K. Huang, Z. F. Yang, J. L. Liu, J. Yu, and J. Ren, "Optimal allocation of virtual inertia for improving small-signal stability," *Proc. CSEE*, vol. 40, no. 3, pp. 713–723, Feb. 2020.

[17] M. Garmroodi, D. J. Hill, G. Verbic, and J. Ma, "Impact of tie-line power on inter-area modes with increased penetration of wind power," *IEEE Trans. Power Syst.*, vol. 31, no. 4, pp. 3051–3059, Jul. 2016.

[18] P. Dey, A. Saha, P. Srimannarayana, A. Bhattacharya, and B. Marungsri, "A realistic approach towards solution of load frequency control problem in interconnected power systems," *J. Electr. Eng. Technol.*, vol. 17, no. 2, pp. 759–788, Mar. 2022, doi: 10.1007/s42835-021-00913-3.

[19] J. Ma, Y. Qiu, and Y. N. Li, "Research on the impact of DFIG virtual inertia control on power system small-signal stability considering the phase-locked loop," *IEEE Trans. Power Syst.*, vol. 32, no. 3, pp. 2094–2105, Feb. 2017.

[20] J. J. Zhao, W. S. Hong, C. S. Xu, and C. L. Xu, "Control strategy of DFIG wind power generation on frequency control of micro-grid based on eigenvalue analysis," *Proc. CSEE*, vol. 37, no. 19, pp. 5613–5621, Oct. 2017.

[21] J. Huang, Z. Yang, J. Yu, J. Liu, and X. Wang, "Optimization for DFIG fast frequency response with small-signal stability constraint," *IEEE Trans. Energy Convers.*, vol. 36, no. 3, pp. 2452–2462, Sep. 2021.

[22] L. Peijie, W. Hua, and B. Xiaoqing, "Small-signal stability constrained optimal power flow based on NLSDP," *Proc. CSEE*, vol. 33, no. 7, pp. 69–76, Apr. 2013.

[23] A. T. Saric and A. M. Stankovic, "Rapid small-signal stability assessment and enhancement following changes in topology," *IEEE Trans. Power Syst.*, vol. 30, no. 3, pp. 1155–1163, May 2015.

[24] P. Kundur, *Power System Stability and Control, Book Translation Group, Transactions*. Beijing, China: China Electric Power Press, 2002.

LIMEI LI was born in Hebei, Baoding, China, in October 1982. She received the B.S. degree in automation from the Inner Mongolia University of Technology, Hohhot, in 2006, and the M.S. degree in control theory and control engineering from the University of Science and Technology Beijing, in 2009.

From 2009 to 2020, she was a Senior Electrical Engineer at Inner Mongolia Electric Power Survey & Design Institute Company Ltd. Since 2020, she has been a Professional Teacher in power supply and consumption technology with the School of New Energy and Electric Power, Hohhot Vocational College. She is currently the Head of the Department. She is the author of more than ten articles and five inventions. Her research interests include substation secondary design, power supply technology, secondary equipment, and power automation system research.

HUI JIANG was born in Hebei, China, in March 1995. She received the B.S. degree in electrical engineering and automation from the Business College of Hebei University (BCHU), Baoding, in 2016. She is currently pursuing the M.S. degree in control science and engineering with the Inner Mongolia University of Science and Technology, Inner Mongolia. Her research interest includes comprehensive energy utilization.

PEIHONG YANG was born in Inner Mongolia, China, in July 1980. He received the B.S. degree in automation from the Inner Mongolia University of Science and Technology, Baotou, in 2005, and the M.S. and Ph.D. degrees in power system and automation from North China Electric Power University, Beijing, in 2008 and 2018, respectively.

From 2010 to 2016 and from 2016 to 2020, he was a Teaching Assistant and an Associate Professor, respectively, with the School of Information Engineering, Inner Mongolia University of Science and Technology. Since 2020, he has been a Professor with the School of Information Engineering, Inner Mongolia University of Science and Technology, and the Inner Mongolia Key Laboratory of Solar & Wind Power. He is the author of two books, more than 70 articles, and more than 15 inventions. His research interests include control and analysis in alternate electrical power system with renewable energy sources and synergetic operational optimization for distributed energy systems.

PENGXIANG FAN was born in Inner Mongolia, China, in February 1981. She received the B.S. and M.S. degrees in transportation engineering and resource management from the Inner Mongolia University of Science and Technology, Baotou, in 2006 and 2013, respectively.

From 2006 to 2010, she was an Assistant Engineer with the Baogang Group, Product Department, where she was an Engineer, from 2010 and 2016. Since 2016, she has been a Senior Engineer with the Energy Conservation and Environmental Protection Center, Baogang Group. She is the author of national standards (GB31335) and more than ten articles. Her research interests include energy saving technology, industrial energy consumption analysis, low carbon energy sources, and power trading.

PAN QI was born in Hebei, China, in July 1997. She received the B.S. degree in electrical engineering and automation from the Hebei University of Technology City College, Tianjin, in 2015. She is currently pursuing the M.S. degree in electronic information (control engineering) with the Inner Mongolia University of Science and Technology, Inner Mongolia. Her research interests include the calculation and analysis of the energy flow of electric-heat integrated energy.

LAN KANG was born in Inner Mongolia, China, in January 1966. She received the B.S. degree in physics major from the Inner Mongolia University for Nationalities, Tongliao, in 1989. From 2004 to 2011, she was an Associate Professor with the School of Mining & Coal, Inner Mongolia University of Science and Technology, where she has been a Professor with the School of Mining & Coal, and the Inner Mongolia Key Laboratory of Solar & Wind Power, since 2011. She is the author of more than 20 articles and more than three inventions. Her research interests include analysis and control of the modern electric power systems and integrated energy system analysis.